Int. J. Bio-Inorg. Hybr. Nanomater., 5(4): 279-295, Winter 2016

Removal of uranium (U(VI)) ions using NiO NPs/Ag-clinoptilolite zeolite composite adsorbent from drinking water: equilibrium, kinetic and thermodynamic studies

S. Yekta[1*], M. Sadeghi[2], H. Ghaedi[3], N. Shahabfar[4]

[1] Department of Chemistry, Qaemshahr Branch, Islamic Azad University, Qaemshahr, Iran
[2] Department of Chemistry, Lorestan University, Khorramabad, Iran
[3] Department of Chemistry, Bushehr Branch, Islamic Azad University, Bushehr, Iran
[4] Department of Nuclear Engineering, Radiation Application, Amir Kabir University, Tehran, Iran

Received: 25 September 2016; Accepted: 27 November 2016

ABSTRACT: The present research describes the performance of NiO NPs/Ag-clinoptilolite composite adsorbent for the removal of uranium (U(VI)) ions from drinking water of Dezful city-Iran. Prior to the experiment reactions, Na-clinoptilolite was chemically treated with NaCl, Silver ions (Ag+) and subsequently Nickel (NiO) NPs to prepare NiO NPs/Ag-clinoptilolite. The samples were characterized by SEM, AAS, XRD and FTIR techniques. The removal process of U(VI) ions by the NiO NPs/Ag-clinoptilolite adsorbent was exploited under various conditions including pH, adsorbent dose, the contact time and initial concentration at room temperature. The adsorption isotherm models including Langmuir, Freundlich, Temkin and Hasley were applied. Experimental adsorption isotherm is successfully described by Langmuir model with a maximum adsorption capacity 23.5849 mg of U(VI)/g of NiO NPs/Ag-clinoptilolite. The ICP-AES results indicated that U(VI) was adsorbed on the composite surface active after 60 min at room temperature with a yield 94%. The reaction kinetic information was studied by utilizing pseudo first and second orders kinetic models. The adsorption kinetics was found fit the pseudo-second-order models. Further the evaluation of the thermodynamic parameters such as ΔG^0, ΔH^0 and ΔS^0, denoted that adsorption process of U(VI) was spontaneous and illustrates a physical adsorption properties and exothermic nature of the adsorption.

Keywords: *NiO NPs/Ag-clinoptilolite, Uranium (U(VI)), Removal, Adsorption, Drinking water*

INTRODUCTION

In recent years, the separation process of uranium from diluted water media is considered as an environmental issue that should not be overlooked (Satpati, *et al.*, 2015). Nearly five percent of all known minerals contain uranium as a substantial structural constituent. Uranium is considered as a toxic radioactive element and usually exists in the hexavalent form in the environmental components. Uranium is one of the most dangerous heavy metals in the environment due to its chemical toxicity and radioactivity. As mentioned, uranium (VI) ions are naturally toxic ions and their existence even at trivial levels leads to a serious public

---

(*) Corresponding Author - e-mail: sina.yekta.chem@gmail.com health problem that should be truly handled. Thus, this element is recognized as an emerging contaminant and if find its way into the human body can cause to inexpiable renal injury and in higher levels may lead even to death. Therefore, the sorption of uranium from water media, especially waste waters is of great importance (Babel & Kurniawan, 2003; Chisholm-Brause, *et al.*, 2001). The EPA (Environmental Protection Agency) declares the maximum permissible uranium concentration of 30 ppb in drinking water (Nriagu, *et al.*, 2012). Plus, the permissible daily amount intake of uranium established by WHO (World Health Organization) based on Gilman's studies is 0.6 µg/kg of body weight/day (Milja, *et al.*, 2011). Uranium might enter the water system from both naturally occurring deposits and human activities. For instance some of human being activities which release it to the environment includes: emissions from the nuclear industry, mill tailings, fertilizers that contain uranium and combusting coal and other fuels, (Birke, *et al.*, 2010) plus utilization growth of DU (Depleted uranium the by-product of the enrichment process) phosphate as military arsenals (Dushenkov, *et al.*, 1997; Wazne, *et al.*, 2003; Sidhu, *et al.*, 2010; Abdi, *et al.*, 2014). There are several methods for the removal of uranium ions from water solutions such as chemical membrane (Fathizadeh, *et al.*, 2011), chemical precipitation (Aydin & Soylak, 2007), biological treatment (Shinde, *et al.*, 2012), solvent extraction (Agrawal, *et al.*, 2000), and ion exchange/adsorption (Fan, *et al.*, 2012), biosorption/remediation, chromatographic, electrodeposition, (Dabrowski, *et al.*, 2004), reverse osmosis, and micellar ultrafiltration (Semiao, *et al.*, 2010). But Among these, ion exchange/adsorption is the most significant removal and recognized as an attractive method due to its ability to remove about 98% of uranium from water samples due to its high efficiency, availability of different adsorbents and simplicity of handling (El Aamrania, *et al.*, 2002). To the best of our knowledge, it is noted that uranyl (UO_2^{2+}) ion has been observed to be strongly adsorbed onto many components of soil including clay minerals and metal oxides under appropriate chemical conditions. Thereupon, such materials can be trustfully applied for uranium (VI) separation from water solutions (Babel & Kurniawan, 2003; Chisholm-Brause, *et al.*, 2001; Gupta & Ali, 2004). In the recent years, nickel oxide (NiO) has been widely considered and attracted noticeable attentions regarding to its remarkable catalytic, electrical and magnetic characteristics. Also, they have been exploited in widespread applications namely the production of catalysis, electrochromic films, fuel cell electrodes and gas sensors, battery cathodes, pn heterojunctions, magnetic materials, photovoltaic devices, electrochemical supercapacitors, smart windows and dye-sensitized photocathodes (Teoh & Li, 2012). Furthermore, there are several reported methods for the synthesis of NiO nanoparticle including pyrolysis by microwave, sol gel method, hydrothermal synthesis, laser chemical method, precipitationcalcination method, ultrasonic radiation, mechanochemical processing, carbonyl method, solid-state method, microemulsion method, flame spray pyrolysis (Teoh & Li, 2012). Plus, nanomaterials, having high surface area and outstanding adsorption ability, have attracted the spotlight on themselves to be employed in the research fields of contaminants adsorption and environmental monitoring programs (Zhang, *et al.*, 2010). Moreover, a wide variety of adsorbents have been used for the removal of radionuclides essentially from water media, namely activated carbon (Mellah, *et al.*, 2006), hydrogels (Karadag, *et al.*, 1995), clays (Dent, *et al.*, 1992), silica gels (Dent, *et al.*, 1992; Michard, *et al.*, 1996), and hydrous oxides (Gupta & Venkataramani, 1991). Among those mentioned common adsorbents, the discovery of zeolite materials owning large surface area and similar pores, revealed a new path for the removal of persistent inorganic contaminants (Stephanie, *et al.*, 1999). On the other hand, silicate minerals, especially zeolites and montmorillonites, are applied in water treatment majorly as ion-exchangers and media for slow filtration (Bosco, *et al.*, 2005). It is notable that many silicate minerals have been utilized for the removal of heavy metals from water media under variant experimental conditions (Doula, 2006; Dimirkou, 2007). Among the different types of zeolites, clinoptilolite have been greatly used in water treatment, due to its low cost and superabundance. Further, it possesses large cation-exchange capacity and also is capable of eliminating of high values of heavy metals from polluted water samples. Loading the surface of clinoptilolite with metal oxide nanoparticles leads to a total improvement in adsorption capacity of the modified zeolite (Doula &Dimirkou, 2008; Camacho, *et al.*, 2010). Ag^+ is the only noble mono-positive cation which forms mononuclear species with desirable stability in aqueous media. Beside, silver is considered to have strong influence on the absorption properties of zeolites. For drinking-water treatment, several types of silver nanoparticles coated substrates-materials have been employed for instance Ag/sand (Mahmood, *et al.*, 1993), Ag/zeolite (Matsumura, *et al.*, 2003) and Ag/fibreglass (Nangmenyi, *et al.*, 2009). In the present research, the synthesis and characterization of NiO NPs/Ag-clinoptilolite zeolite as a novel nanocomposite adsorbent and its application for effective removal and adsorption of uranium (VI) from drinking water of Dezful city has been investigated and reported. However to the best of our knowledge, there has been not such study reported in any previous work.

MATERIALS AND METHODS

Materials

The natural clinoptilolite (NCp) zeolite employed in our research was obtained from the region of the West Semnan, Central Alborz Mountains, Iran and its structural properties is as $(Na,K,Ca)_6\ (Si,Al)_{36}\ O_{72}.20H_2O$. Sodium chloride (NaCl), silver nitrate ($AgNO_3$), hydrochloric acid (HCl), nickel nitrate hexahydrate ($Ni(NO_3)_2.6H_2O$) and uranyl nitrate hexahydrate ($UO_2(NO_3)_2.6H_2O$) were purchased from Merck (Merck, Darmstadt, Germany) and Sigma-Aldrich Co. (USA). Deionized water was used throughout the research.

Instrumentation

The characteristics including morphology, particle sizes and elemental composition of the synthesized adsorbents were investigated using a scanning electron microscope (SEM, HITACHI S-300N). Weight percentages of the elements (silver and nickel) were measured by atomic adsorption spectrometry (AAS, PerkinElmer, USA) coupled to a HGA 400 programmer hybrid system and equipped with a hollow cathode lamp at respective wavelength using an acetylene-air flame. The powder X-ray diffraction (XRD) patterns were recorded using a Philips X'pert Pro diffractometer equipped with CuKα radiation at wavelength 1.54056 Å (30 mA and 40 kV) at room temperature. Data were collected over the range 4–80° in 2θ with a scanning speed of 2° min^{-1}. The IR spectra were scanned on a PerkinElmer model 2000 FT-IR spectrometer (USA) in the wavelength range of 400 to 4000 cm^{-1} using KBr pellets. The concentration of uranium in solutions was measured by an inductively coupled plasma atomic emission spectroscopy (ICP-AES, ICP-optima 2001DV, Perkim-Elmer).

Preparation of Na-clinoptilolite

Herein, prior to the process, 5 g of the clinoptilolite zeolite was calcined at 300°C for 2 h in a furnace for the moister and impurities to be eliminated from the surface. The Na-clinoptilolite form was achieved when above noted clinoptilolite chemically treated with 250 ml of 1M sodium chloride (NaCl) at 90°C overnight and then was washed by deionized water several times till the chloride ions was excluded. Eventually, the modified clinoptilolite (sodium-clinoptilolite) was dried at 85°C for 5 h (Sadeghi, *et al.*, 2016).

Preparation of Ag-clinoptilolite

To proceed the procedure, 4.5 g of the pre-prepared Na-clinoptilolite zeolite was introduced to a 50 mL of a 0.1 M silver nitrate ($AgNO_3$) solution and this mixture was magnetically stirred at 60°C for 5 h to accomplish the ion exchange process in which Ag^+ ions were substituted Na^+ ions. The synthesized Ag-clinoptilolite zeolite was further filtered and washed with deionized water and 0.1 M HCl solution to exclude the surplus silver ions from the zeolite framework. Afterwards, this gained product was dried at 110°C for 16 h. Finally, the clean and dry Ag-clinoptilolite zeolite was calcined at 400°C for 4h. This process was reiterated for three times to approach the efficient ion exchange (Sadeghi, *et al.*, 2016).

Preparation of NiO NPs/Ag-clinoptilolite

The impregnation method was applied for preparation of NiO NPs/Ag-clinoptilolite zeolite composite. In a typical experimental process, 3 g of the Ag-clinoptilolite zeolite powder was introduced to a solution of 0.5 M of nickel nitrate hexahydrate ($Ni(NO_3)_2.6H_2O$)

in 250 mL deionized water meanwhile the suspension was vigorously stirred at room temperature for 6h. Then the powder were filtered, washed with distilled water and dried overnight at 110°C . Lastly, after calcination at 550°C in the air for 4h, the attained powder was uncovered as the NiO NPs/Ag-clinoptilolite zeolite composite. Further, the pure NiO NPs was prepared without the presence of zeolite under similar conditions (Sadeghi, *et al.*, 2016).

Adsorption experimental

The standard uranium stock solution was prepared by dissolving an appropriate quantity of uranyl nitrate hexahydrate ($UO_2(NO_3)_2.6H_2O$) in 500 mL of this water. The sample solutions were then prepared from the stock solution. The experiments series using the abovementioned solutions were done at room temperature by stirring of a 20 mL uranium solution with 0.2 g of the added NiO NPs/Ag-clinoptilolite absorbent.

RESULTS AND DISCUSSION

SEM

To establish the morphology and crystalline size of the pre-synthesized clinoptilolite zeolite, Ag-clinoptilolite zeolite, NiO NPs/Ag-clinoptilolite zeolite composite and pure NiO NPs, SEM analysis were applied as depicted in Fig. 1. The SEM images demonstrate the homogeneous morphology of the structures of clinoptilolite (1a) and Ag-clinoptilolite (1b) zeolites and NiO nanoparticles deposited on the surface of Ag-clinoptilolite zeolite (1c and d). They further express that Ag ion exchange and NiO NPs loading processes had no negative influence on the morphologies and the crystallinity of the structures as they maintained in good status. Also the average crystalline size of NiO NPs in the composite was proved to be in nanometric dimensions (less than 100 nm). Moreover, it is should be emphasized that NiO NPs loaded on the zeolite has lower crystalline size than that of pure NiO NPs (1e).

AAS

The amounts of silver and nickel elements in the adsorbent catalyst were determined through elemental analysis by atomic absorption spectrometry (AAS). The results revealed that the amounts of silver and nickel were 6.4 wt% and 17.2 wt%, respectively.

XRD

In Fig. 2, XRD patterns of the clinoptilolite zeolite, Ag-clinoptilolite zeolite, NiO NPs/Ag-clinoptilolite zeolite composite and pure NiO NPs have been represented, respectively. As can be observed from the patterns, the sharp peaks corresponded to clinoptilolite zeolite occurred at (2θ) of 11.3993°-74.1895° (Fig.

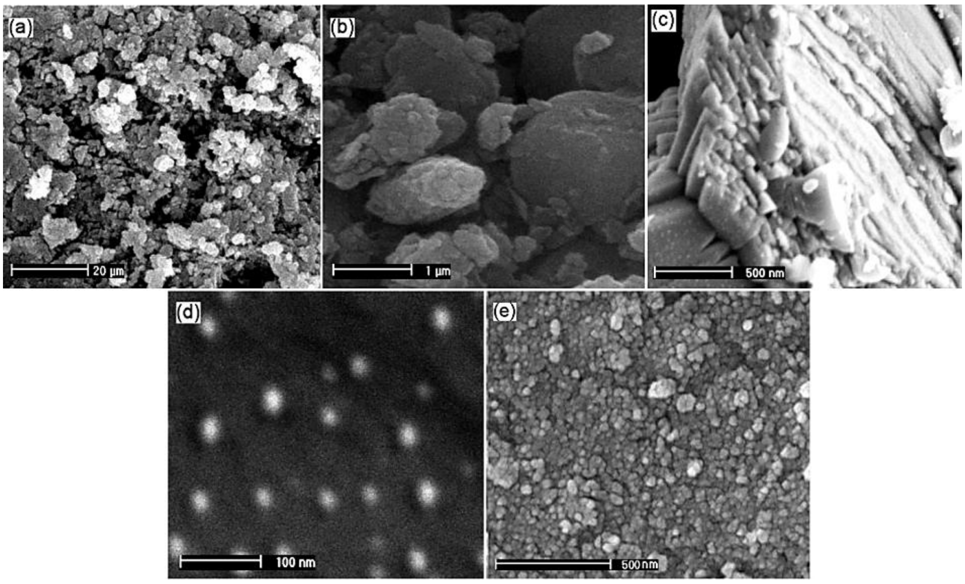

Fig. 1. SEM images of the zeolite samples: (a) clinoptilolite, (b) Ag-clinoptilolite, (c) and (d) NiO NPs/Ag-clinoptilolite and (e) pure NiO NPs

3a) and are in good agreement with those of the clinoptilolite zeolite with Joint Committee on Powder Diffraction Standards (JCPDS: 00-025-1349). Fig. 2b shows the clinoptilolite zeolite structure was maintained after silver cation exchange in the Ag-clinoptilolite. Moreover, the synthesized NiO NPs as guest material were loaded as a 17.2 wt% of unit on the Ag-clinoptilolite zeolite as the host material, caused a series of three new peaks which were occurred at 2θ of 37.4823°, 43.3248° and 63.1107° referring to the diffraction planes of (111), (200) and (220) respectively which are in good consistency with those of NiO NPs. Meanwhile, no characteristic peaks affiliated to the impurities existence were detected in the patterns during NiO species loading. These demonstrated peaks as red points in Fig. 2c show that NiO NPs have been dispersed and deposited onto the Ag-clinoptilolite and meanwhile reveal a host-guest interaction between Ag-clinoptilolite zeolite framework and NiO NPs. A definite line broadening of the scattering pattern in Fig. 2c is an explanation upon which the synthesized NiO particles can be accounted in nanoscale scope. Though, a poor loss of crystallinity is seen in Fig. 2b related to the lower intensity of the peaks. This may be due to the dealumination of Ag-clinoptilolite zeolite and NiO NPs/Ag-clinoptilolite zeolite composite and affiliated to the location of impregnated nickel and substituted silver cations. The Ni^{2+} ions within the zeolite framework can interact with the aluminate sites more strongly than that of Na^{+} or Ag^{+} ions. It can be inferred that with silver ion exchange in clinoptilolite zeolite and subsequent loading of NiO NPs onto Ag-clinoptilolite, the structure of the zeolites did not change. As a matter of fact, the capacity of the clinoptilolite zeolite to possess the guest species is bounded. Thus, the adsorption capability of the host cations (Si, Al and Na) will be ceased if the capacity is saturated. In contrast, the amount of the host species in the Ag-clinoptilolite grows as the nickel oxide content raises. The applied NiO NPs were dispersed-deposited on the surface of Ag-clinoptilolite. Though, because of the relative aggregation while processing of the noted composite, some particles are too large to sit inside the structure. Thereupon, high loading of NiO NPs will lead to unwelcome structural damage to the zeolite framework. Also, the size of the prepared NiO NPs deposited on the Ag-clinoptilolite was also surveyed via XRD and line broadening of the peak at 2θ= 0°-80° employing Debye-Scherrer equation (2) :

$$d = \frac{0.94\lambda}{\beta \cos\theta} \tag{2}$$

Where d refers to the crystal size, β is the full width at half maximum (FWHM), λ is the wavelength of X-ray source and θ is Bragg diffraction angle. The peaks related to the pure NiO NPs observed at scattering an-

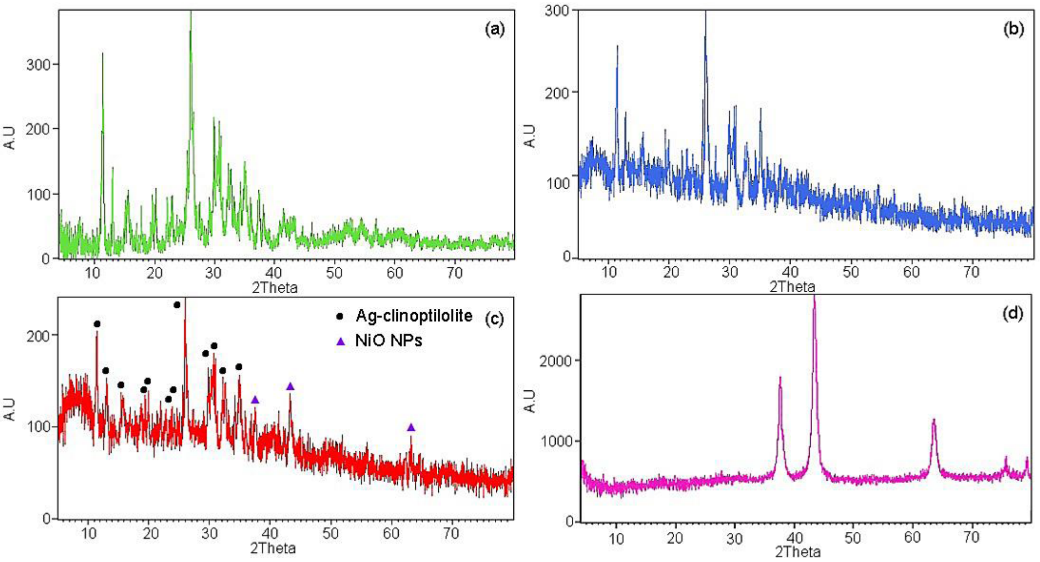

Fig. 2. XRD patterns of the zeolite samples: (a) clinoptilolite, (b) Ag-clinoptilolite, (c) NiO NPs/Ag-clinoptilolite and (d) pure NiO NPs

gles (2θ) of 37.4823°, 43.3248°, 63.1107°, 75.3154° and 79.4361° attributed to the diffraction planes of (111), (200), (220), (311), and (222), respectively which have been crystallized in the monoclinic phase and are in good consistency with those of NiO NPs with JCPDS:01-073-1523. Applying this equation, the average particle size for NiO NPs in the NiO NPs/Ag-clinoptilolite zeolite composite and pure NiO NPs are calculated to be 24.2 nm and 48.6, respectively. The particle size achieved from XRD measurement is in good agreement with the results from the SEM study.

FTIR

The characterization of the as-prepared adsorbents accompanied with the clinoptilolite zeolite precursors were further perused via FT-IR spectra as depicted in Fig. 3. Peak positions are nearly similar for three samples. It should be highlighted that all of the three typical samples, including clinoptilolite zeolite and as-synthesized Ag-clinoptilolite and NiO NPs/Ag-clinoptilolite composite show peaks around 465 cm^{-1} and 524 cm^{-1} which are attributed to the bending vibrations of the insensitive internal TO_4 (T= Si or Al) tetrahedral units and double six rings (D6R) external linkage within the clinoptilolite zeolite structure, respectively. Also, the peaks occurred at 674 cm^{-1} and 797 cm^{-1} are corresponded to the external linkage and internal tetrahedral symmetrical stretching vibrations, respectively. Furthermore, the peaks around 1034 cm^{-1} are assigned to the external linkage and internal tetrahedral asymmetrical stretching vibrations, and peaks at around 1635 cm^{-1}, 3437 cm^{-1} and 3623 cm^{-1} are affiliated to H–O–H bending O–H bonding (hydroxyl groups) vibrations and discrete water absorption bands of the clinoptilolite, respectively. Having observed the Fig. 3a-3c it can be confirmed that no significant alteration has come about in the bands of Ag-clinoptilolite zeolite and NiO NPs/Ag-clinoptilolite zeolite composite compared with the original clinoptilolite zeolite, which tends to lend further support to the idea that the ion exchange treatment of clinoptilolite zeolite by silver ion and nickel oxide has trivial effect on the chemical structure of the zeolite framework. Moreover, Fig. 3c shows a new peak assigned to the synthesized loaded NiO NPs. The absorption peak at 908 cm^{-1} is attributed to Ni–O–Si and Ni–O–Al bonds and pointed the trapped nickel in the structure of zeolite. In Fig.3d, the absorption peak at 420 cm^{-1} refers to Ni–O bond. The peaks around 1672 cm^{-1} and 3416 cm^{-1} are affiliated to H–O–H bending and O–H bonding (hydroxyl groups possibly related to Ni-OH bond) vibrations of the adsorbed water on the surface of the NiO NPs, respectively.

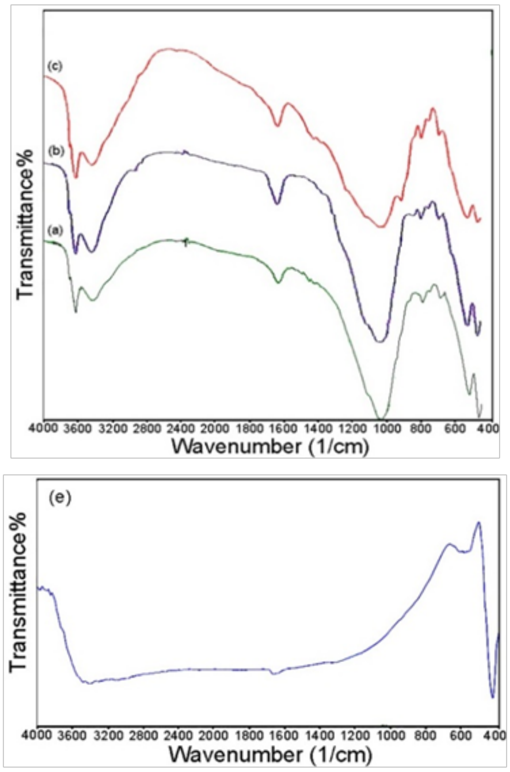

Fig. 3. FTIR spectra of the sythesized samples: (a) clinoptilolite, (b) Ag-clinoptilolite, (c) NiO NPs/Ag-clinoptilolite and (d) pure NiO NPs

Removal and adsorptive properties study

U(VI) containing solution was prepared by dilution of pre-prepared stock solution. The optimized dose of 0.2 g of NiO NPs/Ag-clinoptilolite added in a 20 mg/L of U(VI) (optimized values) Erlenmeyer flask and stirred rapidly for 60 min as selected optimized time at room temperature. Then, the composite adsorbent was separated from supernatant by centrifuging the solution. In order to investigate the removal of U(VI), the adsorption behavior of NiO NPs/Ag-clinoptilolite was assessed and those progresses were controlled by ICP-AES technique. Also the effects of several operational parameters such as pH, adsorbent dose, contact time and initial concentration, and also kinetics and thermodynamic reactions were considered.

Effect of pH

The role of pH on the removal and adsorption yield of U (VI) ions on NiO NPs/Ag-clinoptilolite adsorbent was surveyed by using uranium solution of 20 mg/L at pre-optimized temperature (25°C) for 60 min. The influence of initial pH parameter on the adsorption and removal process has been demonstrated in Fig. 4. As can be seen in Fig. 4, the adsorption of uranium on the adsorbent varied significantly with changing the pH of solution. It should be noted that the metal chemistry in the solution along with ionization state of modifying agents which related to the availability of adsorptive sites highly depends on pH. In this work, the adsorption procedure of uranium ions was investigated in the pH range of 2-8. At low pHs, UO_2^{2+} existed in an acidic solution. The uranium ions retention was significantly decreased at low pH ranges because of the intense interaction of H^+ ions with the adsorptive sites of NiO NPs/Ag-clinoptilolite adsorbent than that of U(VI) ions. Therefore, protonation of adsorbent in strong acidic conditions lessens the available ionized groups and target ions tendency to be adsorbed. Also at high pH ranges, concentration of negative charge density on the adsorbent surface increases and it is possible for UO_2^{+2} to be hydrolyzed to different forms of uranium hydroxide complexes such as $UO_2(OH)_2$, $(UO_2)_2(OH)_2^{2+}$, $(UO_2)_3(OH)_5^+$ due to excess of OH ions in basic media results in a decrease of U(VI) adsorption by mentioned adsorbent (Schmeide, *et al.*, 2000). Thus, it is essential to find the best pH value to reach the high yield adsorption-removal process. The most selectivity and removal 94% gained at optimized pH equal 4. The solution pH was adjusted via 1M solutions of NaOH and HNO_3. Finally, the supernatant solution of U(VI) were brought out and introduced to the ICP-AES.

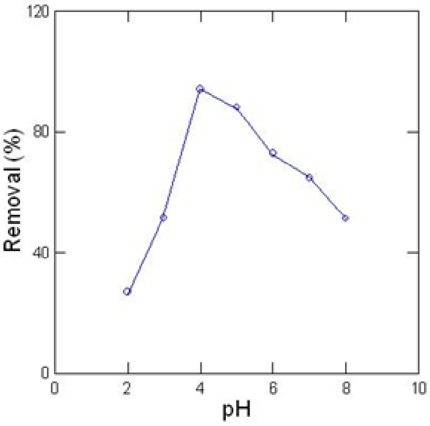

Fig. 4. The effect of pH on the removal efficiency of U(VI) by NiO NPs/Ag-clinoptilolite

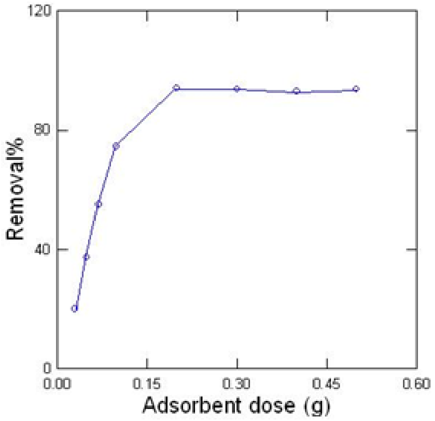

Fig. 5. The effect of adsorbent dose on the removal efficiency of U(VI) by NiO NPs/Ag-clinoptilolite

Effect of adsorbent dose

The selection of optimized dosage of an adsorbent is of great importance in any sort of scientific analytical research because one of the main factors that make a new adsorbent attractive and also reliable is to use the least dose of it for the most value of adsorption and removal. In this study, to find the best and optimized adsorbent dose for the removal of uranium ions, the adsorption properties of U(VI) was surveyed at range of 0.03-0.5 g of NiO NPs/Ag-clinoptilolite. As illustrated in Fig. 5, the more the dose of adsorbent, the better the removal efficiency, until the point after which no more sensible variations is occurred and the curve slope tend to a linear form which implies constant values. Eventually, the value of 0.2 g was considered as the appropriate dose for NiO NPs/Ag-clinoptilolite to carry out high yield removal and adsorption process.

Effect of contact time

The effect of different time intervals on the adsorption process of U(VI) on NiO NPs/Ag-clinoptilolite was carried out. These series of experiments provide a sensible comparison between adsorption ability of adsorbent. Fig. 6 represents the variation of adsorption value (%) with shaking time and also the reliability of adsorption yield of uranium ions on the NiO NPs/Ag-clinoptilolite adsorbent to the contact time. The adsorption time was investigated in the scope of 10-

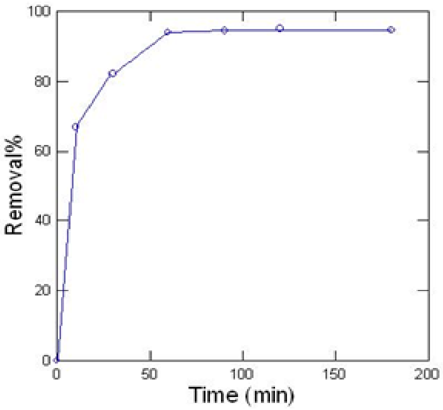

Fig. 6. The effect of contact time on the removal efficiency of U(VI) by NiO NPs/Ag-clinoptilolite

180 min. As the reaction process went on and time increased, the adsorption increased rarely up to 60 min and then remained in constant value. Therefore, to nail a shorter analysis period of time 60 min was considered as optimum value.

Effect of initial concentration

The effect of initial U(VI) concentration in the range of 20 to 500 mg/L on the adsorption was investigated and is shown in Fig. 7. It is evident from the Fig that the percentage U(VI) removal decreased with the increase in initial concentration of U(VI) due to the fixed quantity of adsorbents used in this study. The initial U(VI) concentration provides the necessary driving force to overcome the resistance to the mass transfer of U(VI) between the aqueous phase and the solid phase. The increase in initial U(VI) concentration also enhances the interaction between U(VI) and NiO NPs/Ag-clinoptilolite. Therefore, an increase in initial concentration of U(VI) enhances the adsorption uptake of U (VI). This is due to the increase in the driving force of the concentration gradient with the increase in the initial U(VI) concentration. While the percentage uranyl ions removal was found to be 94.1% for 20 mg/L of initial concentration, this value was 61.9% for that of 500 mg/L.

Adsorption isotherms study

Adsorption is known as a separation procedure in which some materials, so-called adsorbate is concentrated from a liquid phase or bulk vapor on the surface area of a porous solid (adsorbent). Commonly the adsorbed amount is only a fraction of a monolayer. Therefore, to adsorb a significant amount of material so-called analyte, the adsorbent must have a large particular surface area. The particular surface area of typical adsorbents range from 0.1 to 1.0 km^2/kg, i.e. the area of a football field in a kg of adsorbent (Adamson *et al.*, 1990). In present research, different kinds of adsorption isotherm models were applied via analyzing solutions in contact with NiO NPs/Ag-clinoptilolite to Figure out the affinity between the equilibrium concentrations in the liquid and solid phases before and after experiment. The equilibrium adsorption isotherms are described by various Langmuir, Freundlich, Temkin and Hasley models in below. The sorption isotherms were investigated in drinking water of Dezful city as pH= 4, temperature (25°C), and different initial solution concentrations pertain to the six various concentrations of 20 to 500 mg/L.

Langmuir isotherm

This model refers that the adsorption procedure takes place at a particular adsorption surface area. The attraction between analytes and the active sites of adsorbent decreases as the operative surface is saturated by target ions. Normally the adsorbed amount of matter is measured as a function of the partial pressure or concentration at a certain given temperature and the result explained as an adsorption isotherm. There are several types of adsorption models, but the Langmuir adsorption isotherm model is the most common between them (Adamson, *et al.*, 1990). Langmuir's isotherm demonstrating the adsorption process of adsorbate on the surface of the adsorbent requires three basic assumptions that insinuated before: First; the ad-

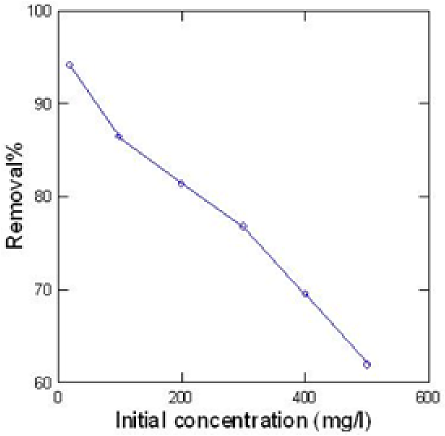

Fig. 7. The effect of initial concentration on the removal efficiency of U(VI) by NiO NPs/Ag-clinoptilolite

sorbent surface is in contact with a solution containing an adsorbate that is strongly attracted to the surface. Second; surface has a particular number of active sites in which the solute molecules can be adsorbed. Third; the adsorption includes the junction of just one layer of molecules to the surface, i.e. monolayer adsorption (Duff David, *et al.*, 1988). Thus, Langmuir adsorption isotherm is commonly applied to illustrate the maximum adsorption capacity of considered adsorbent and also impress single coating layer on adsorption surface. Langmuir isotherm can be represented in the form of the following equation (2) (Duff David, *et al.*, 1988).

$$\frac{1}{q_m} = \frac{1}{K_L q_m} \times \frac{1}{C_e} + \frac{1}{q_m} \qquad (2)$$

Where q_m implies the maximum U(VI) uptake per unit mass of adsorbent, K_L (mg/g) is constant assumed value and C_e is the equilibrium concentration of the adsorbent. The plot $1/q_m$ versus $1/C_e$ is represented in Fig. 8. Also, the separation factor, RL known as a dimensionless constant, representing the status of the Langmuir isotherm toward a certain adsorption process has been calculated from equation (3) (Freundlich, 1906):

$$R_L = 1/(1 + K_L.C_0) \qquad (3)$$

Where, C_o is defined as the initial concentration of analyte and K is a constant value for Langmuir isotherm. It should be considered that the desirable value for above mentioned parameter is $0 < R_L < 1$, and other possible responses such as R_L=0, R_L =1 and R_L >1 show that the isotherm is irreversible, linear and undesirable for each case, respectively.

Freundlich isotherm

The Freundlich isotherm is usually used for modeling the adsorption on heterogeneous surfaces and also applied for the trace concentration. It proposes that the sorption is not confined to one specific class of the sites and assumes surface heterogeneity. Freundlich model is represented by the following equations (4 and 5) (Hall, *et al.*, 1966):

$$q_e = K_F C_e^{\frac{1}{n}} \qquad (4)$$

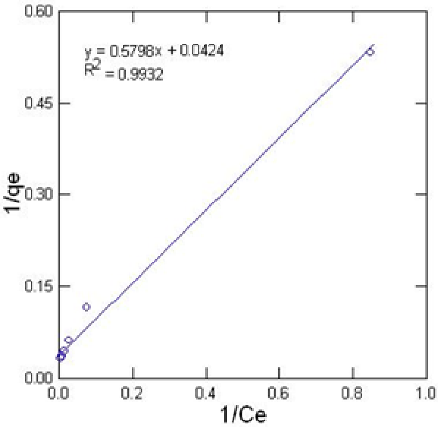

Fig. 8. The Langmuir isotherm plot related to the adsorption process of U(VI) by NiO NPs/Ag-clinoptilolite (pH: 4, adsorbent dose: 0.2g, contact time: 60 min)

$$\log q_e = \log K_F + \frac{1}{n} \log C_e \qquad (5)$$

Where K_F is the constant of Freundlich model [(mg/g)/(mg/L)] and n is a parameter refers to adsorption tendency determined from the intercept and slope of the plot. Fig. 9 shows the plot of this isotherm that gives a straight line of slope ln q_e versus C_e.

Temkin isotherm

The Temkin isotherm suggests a linear decease of sorption energy and can be expressed via the following equation (6) (Temkin, 1941):

$$q_e = \beta \ln \alpha + \beta \ln C_e \qquad (6)$$

Here α and β are Temkin adsorption con-

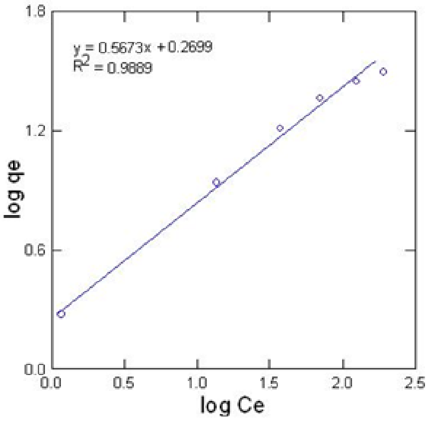

Fig. 9. The Freundlich isotherm plot for the adsorption of U(VI) by NiO NPs/Ag-clinoptilolite (pH: 4, adsorbent dose: 0.2g, contact time: 60 min)

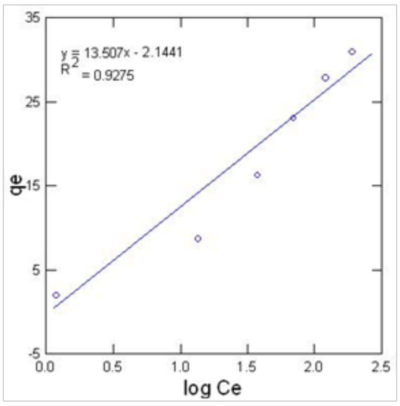

Fig. 10. The Temkin isotherm plot for the adsorption of U(VI) by NiO NPs/Ag-clinoptilolite (pH: 4, adsorbent dose: 0.2g, contact time: 60 min)

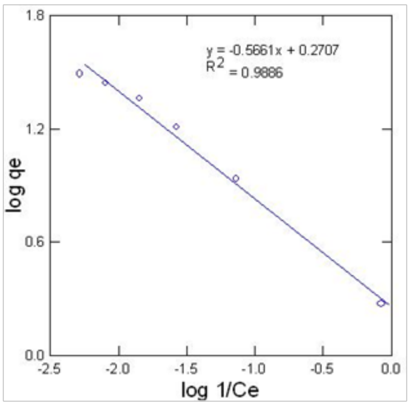

Fig. 11. The Hasley isotherm plot for the adsorption of U(VI) by NiO NPs/Ag-clinoptilolite (pH: 4, adsorbent dose: 0.2g, contact time: 60 min)

stants. Fig. 10 reveals the plot of this isotherm that gives a straight line of slope q_e versus ln C_e.

Hasley isotherm

The Hasley isotherm model can be utilized to evaluate the multilayer adsorption for the adsorption of U(VI) at a relatively large distance from the surface. Herein we discuss this isotherm model with equilibrium equation below (7) (Hasley, 1952):

$$\log q_e = \left[\left(\frac{1}{n_H}\right)\log(K_H)\right] - \left(\frac{1}{n_H}\right)\log\left(\frac{1}{C_e}\right) \qquad (7)$$

n_H and K_H parameters are Hasley isotherm constants and were calculated from the slope and intercept of the linear plot based on ln q_e versus ln($1/C_e$) respectively and its plot is shown in Fig. 11. The correlation coefficient (R^2) successfully implied the consistency between experimental data and the model predicated values. A relatively high R^2 value proves that the model desirably demonstrates the adsorption isotherm. According to the R^2 value, high regression correlation coefficient was recognized in appropriate straight linear with the Langmuir (R^2=0.9932) isotherms as compared to the Freundlich (R^2=0.9889), Temkin (R^2=0.9275) and Hasley (R^2=0.9886) isotherm models. The data related to these models are summarized and listed in Table 1.

Adsorption kinetics study

The adsorption kinetics is of great importance specifically for designing the adsorption systems and also for providing optimum operating conditions for adsorption reaction study. The kinetic investigations are performed especially for three major reasons: measuring the rates of reaction under different experimental con-

Table 1. Different adsorption isotherm model factors results for the adsorption of U(VI) by NiO NPs/Ag-clinoptilolite (T=25°C, pH: 4, adsorbent dose: 0.2g, contact time: 60 min)

Isotherm Type	Isotherm parameters	
Langmuir	K_L = 0.0731(L/mg) q_m = 23.584(mg/g) R_L = 0.0264	R^2 = 0.9932
Freundlich	K_F = 1.8616(mg/g) (L/mg) n = 1.7627	R^2 = 0.9889
Temkin	α = 1.4411 (g/mg) β = 13.507 (mol^2/KJ^2)	R^2 = 0.9275
Hasley	K_H = 3.0067(L/mg) n_H = 1.7664	R^2 = 0.9886

ditions, the determination the effect of concentration and temperature on reaction rates, and also for determination of the required time for achieving the equilibrium during the adsorption procedure. The samples for adsorption kinetics study were prepared by adding 0.2 g of NiO NPs/Ag-clinoptilolite at pH= 4 and the U(VI) ions concentration was 20 mg/L, in separate containers, at 298 oK, At certain time intervals. After samples were collected using a 0.45 mm membrane filters and then analyzed by an atomic adsorption spectroscopy. The uranium ions adsorption value at time t, q_t (mg/g), was calculated by following equation (8):

$$q_t = (C_0 - C_e)V / W \tag{8}$$

Where C_0 and C_t are the U(VI) concentrations in the original solution and after passing of time t, respectively. The volume of the solution V, and W represents the weight of the NiO NPs/Ag-clinoptilolite used. The adsorption kinetics of U(VI) ions onto the above mentioned adsorbent, measured by using Pseudo-first-order and pseudo-second-order models (Christian, *et al.*, 2003; Monoj, 2010).

Pseudo-first-order model

The equation (9) represents this model is:

$$\log(q_e - q_t) = \log q_e - \frac{k_1}{2.303} t \tag{9}$$

Where q_e and q_t (mg/g) refer to the adsorption capacity of U (VI) ions at equilibrium and at time t, respectively, k_1 is the pseudo-first-order constant (min^{-1}). The values of q_e and k_1 were specified from the intercept and slope of Fig. 12, respectively. $\log(q_e-q_t)$ was also plotted versus time interval, a straight line should be obtained with a slope of k_1, if the first-order kinetics is credible (Lagergern, 1898).

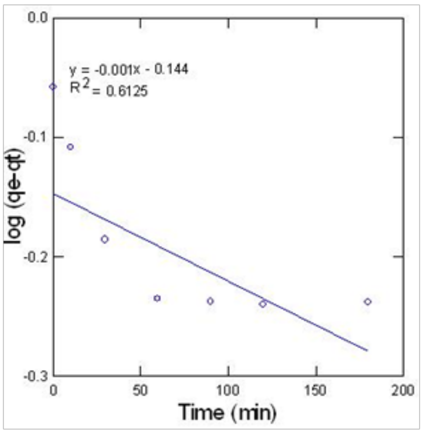

Fig. 12. Plot of pseudo-first-order for the adsorption of U(VI) on the NiO NPs/Ag-clinoptilolite

Pseudo-second-order model

(McKay, 1998) proposed a pseudo second order model for the adsorption of divalent metal ions onto sorbent particles that is following below equation (10):

$$\frac{t}{q_t} = \frac{1}{k_2 q_e^2} + \frac{t}{q_e} \tag{10}$$

Where q_e and q_t are the amounts of U(VI) ($g \bullet mg^{-1}$) at equilibrium and other time intervals. k_2 implies the rate constant of the pseudo second order equation ($g \bullet mg^{-1} min^{-1}$). When the second order model is an appropriate expression, a pattern of t/q_t against time (t) will attain a linear result with a slope of 1/q and an excise of $1/k_2 q_e^2$. The adsorbed amounts (q) of U(VI) were calculated using the following equation (11):

$$q = \frac{(C_o - C_e) \times V}{m} \tag{11}$$

Where C_o and C_e refer to the initial and equilibrium concentrations of U(VI) ($g \bullet mg^{-1}$) in the liquid phase, respectively, V is the volume of solution (Liter) and also m is the mass of adsorbent (gram). The pattern among versus time t and the pattern of t/q versus time t applied for determination of rate constant of pseudo first order and pseudo second order of the adsorption and correlation coefficient (R^2). In Fig. 13, plot of Pseudo-first-order kinetic is represented. From Figs 12 and 13, and the result data in Table. 2, represent that the

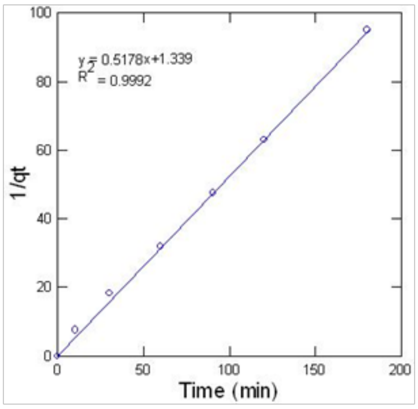

Fig. 13. Plot of pseudo-second-order for the adsorption of U(VI) by NiO NPs/Ag-clinoptilolite

Table 2. The different kinetics model rate constants for the adsorption of U (VI) by NiO NPs/Ag-clinoptilolite (T=25°C, pH: 4, adsorbent dose: 0.2g, initial concentration: 20 mg/L)

Kinetic Model Type	k_1 (min^{-1})	k_2 ($g.mg^{-1}.min^{-1}$)	R^2
First-order	0.0023	-	0.6125
Second-order	-	0.2007	0.9992

pseudo-second-order model is the best fitting model because it provides higher correlation coefficient (R^2=0.9992) than pseudo-first-order model (R^2= 0.6125). Thus, upon the obtained results the U(VI) ions adsorption on NiO NPs/Ag-clinoptilolite is followed via pseudo second order.

Adsorption thermodynamic study

Effect of Temperature

In present study, the removal and adsorption of U(VI) on the NiO NPs/Ag-clinoptilolite was investigated in the temperature range of 25-50°C under pre-determined optimized conditions. The related results are depicted in Figs. 14 and 15. Fig. 14 illustrates the effect of temperature on the removal of uranium ions on the composite adsorbent surface. As can be obviously found, the adsorption of U(VI) on the NiO NPs/Ag-clinoptilolite undergoes decrease as the temperature increases slowly. This happens because the formed bonds between uranium ions and active sites of nanocomposite adsorbent being loosed and broken as a result of raising reaction temperature. To evaluate the thermodynamic characteristics, various solutions were prepared with initial U(VI) concentration in the scope of 20 mg/L, pH 4 and then added 0.2 g NiO NPs/Ag-clinoptilolite to each solution. Then the prepared samples were mounted on a stirrer and the solution stirred continuously for 60 min at 298-328 oK, respectively. Next, the suspension solutions were filtered using a 0.45 mm membrane and the filtrates were measured using an atomic adsorption spectroscopy immediately. The amount of adsorbed U(VI) by present used adsorbent can be determined by considering the variations between the initial and the equilibrium U(VI) concentrations. To determine the process of spontaneous reaction, energy and entropy parameters should be noticed. Plus, the dependence of distribution ratios on the temperature was surveyed. The correlation between K and Gibbs free energy ΔG^0 variation in sorption has been presented in below (12):

$$\Delta G^0 = -RTLnK_d \tag{12}$$

Where R is the universal gas constant (8.314 $J.mol^{-1}.K^{-1}$), T is the absolute temperature in kelvin (°K) and K_d is the distribution coefficient. Gibbs free energy variation can also be considered in terms of enthalpy variation, ΔH^0, entropy variation, ΔS^0, as mentioned in following equation (13):

$$\Delta G^0 = \Delta H^0 - T\Delta S^0 \tag{13}$$

A new explanation is gained by integration (12 and 13) as is depicted in following (Vans Hoff equa-

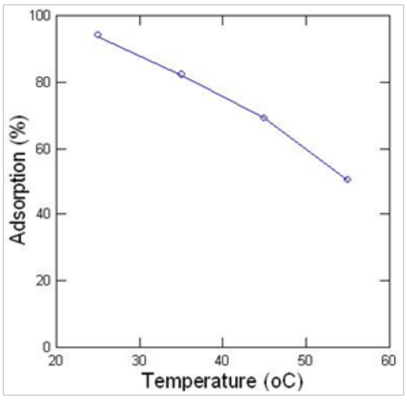

Fig. 14. Plot of U(VI) adsorption% versus temperature (°C)

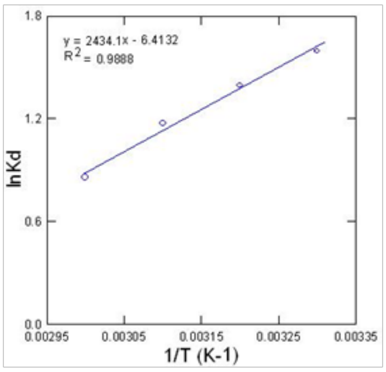

Fig. 15. Plot of Vans Hoff (ln K_d versus 1/T) for the adsorption of U(VI) by NiO NPs/Ag-clinoptilolite at different temperature

Table 3. Thermodynamic function values for the adsorption of U(VI) by NiO NPs/Ag-clinoptilolite (pH: 4, adsorbent dose: 0.2 g, contact time: 60 min, initial concentration: 20 mg/L)

Temperature (°K)	ΔG^0 (KJ/mol)	ΔH^0(KJ/mol)	ΔS^0(J/mol.K)	R^2
298	-3.9514	-20.2371	-53.3193	0.9888
308	-3.5675			
318	-3.0959			
328	-2.3386			

Table 4. Comparison of adsorption capacity of the NiO NPs/Ag-clinoptilolite for U(VI) with different adsorbents

Adsorbent Type	Adsorption isotherm	(mg/g)	References
AC-Fe_3O_4 nanocomposite	Langmuir	15.87	Akbari Jonoush *et al*., 2015
Zeolite-iron oxide magnetic nanocomposite	Langmuir	22.40	Fungaro *et al*., 2012
Orange peel	Langmuir	16.12	Mahmoud *et al*., 2013
Quercetin modified Fe_3O_4 nanoparticles	Langmuir	12.33	Sadeghi *et al*., 2012
Ammonium-modified Zeolite	Langmuir	2.056	Bakatula *et al*., 2015
Manganese oxide coated zeolite	Langmuir	15.1	Runping *et al*., 2007
NiO NPs/Ag-clinoptilolite	Langmuir	23.58	This study

tions (14 and 15)):

$$\ln K_d = -\frac{\Delta H^0}{R} \times \frac{1}{T} + \frac{\Delta S^0}{R} \qquad (14)$$

$$K_d = \frac{q_e}{C_e} \qquad (15)$$

Furthermore, both the enthalpy (ΔH^0) and the entropy (ΔS^0) of adsorption process can be indicated from the slope and the intercept of the linear fits which are gained by drawing ln K_d against 1/T respectively. The negative values ΔG^0 show that the adsorption process is spontaneous with attachment of uranium ions to the composite adsorbent. Based on data results the adsorption of U (VI) on the NiO NPs/Ag-clinoptilolite would be attributed to a physical adsorption procedure (ΔH^0 = 20.2371 KJ/mol). Therefore, the enthalpy variation following adsorption is negative which means the exothermic nature of adsorption. The entropy variations of the system along with the adsorption of uranium ions on the NiO NPs/Ag-clinoptilolite is positive in all cases explaining that more discovery is generated following adsorption and reflects that no particular change takes place in the internal structure of ocomposite during adsorption of U(VI). The plots data of versus 1/T is shown in Fig. 15, and data results are represented in Table. 3. Table. 4 denotes the comparison of the adsorption capacity of NiO NPs/Ag-clinoptilolite for U(VI) and the isotherm model with other materials. Based on this table, it can be concluded that NiO NPs/Ag-clinoptilolite has important potential for the removal of U(VI) from water samples.

CONCLUSIONS

The present research is focused on the preparation of NiO NPs/Ag-clinoptilolite adsorbent through two facile routes sol-gel and indirect methods and applied for effective removal of U(VI) ions from water sample of Dezful city. The prepared adsorbents were characterized by SEM, AAS, XRD and FT-IR analyses and the removal process followed via inductively coupled plasma atomic emission spectroscopy (ICP-AES) technique. Also, different conditions such as pH, adsorbent dose, the contact time and initial concentration at room temperature were investigated and optimized to approach the highest adsorption/removal efficiency of U(VI) ions. Adsorption isotherms including Langmuir, Freundlich, Temkin and Hasley have been analyzed to the equilibrium data. The Langmuir isotherm was found to well represent the measured adsorption data. The parameters including: pH=4, adsorbent dose (0.2 g), contact time (60 min) and temperature (25°C) were considered as optimized conditions for this process. The experimental results revealed that NiO NPs/Ag-clinoptilolite leads to maximum removal and adsorption of U(VI) from water sample. On the other hand, the reaction kinetic information was surveyed utilizing pseudo-first and pseudo-second orders kinetic models. Besides, the adsorption kinetics of U(VI) was matched nicely with the pseudo-second-order kinetic model. Then, thermodynamic study for the adsorption reactions was evaluated and the results showed that by increasing the temperature, efficiency reaction decreased. Thereupon, the NiO NPs/Ag-clinoptilolite composite show promising application as an appropriate adsorbent for removal of uranium ions from water samples.

ACKNOWLEDGMENT

The authors give their sincere thanks to the Islamic Azad University, Ahvaz Iran, Islamic Azad University, Qaemshahr Iran and Islamic Azad University, Bushehr Iran.

REFERENCES

Abdi, M.R.; Shakur, H.R.; Rezaee Ebrahim Saraee, Kh.; Sadeghi, M.; (2014). Effective Removal of Uranium Ions from Drinking Water Using CuO/X Zeolite Based Nanocomposites: Effects of Nano Concentration and Cation Exchange. J. Radioanal. Nucl. Chem., 300 (3): 1217-1225.

Adamson, A.W.; (1990). Physical Chemistry of Surfaces. 5th Ed., John Wiley & Sons, New York.

Agrawal, Y.K.; Shrivastav, P.; Menon, S.K.; (2000). Solvent Extraction, Separation of Uranium (VI) with Crown Ether. Sep. Purif. Technol., 20 (2-3): 177–183.

Akbari Jonoush, Z.; Farzadkia, M.; Naseri, S.; Mohajerani, H.R.; Esrafili dizaji, A.; Shahamat Dadban, Y.; (2015). Removal of Uranium (VI) from Aqueous Solution by Uranium Benzamide Complex Using AC-Fe3O4 Nanocomposite. Iran. J. Health & Environ., 7 (4): 499-510.

Annadurai, G.; Juang, R.S.; Lee, D.J.; (2002). Use of Cellulose-Based Wastes for Adsorption of Dyes from Aqueous Solutions. J. Hazard. Mater., 92 (3): 263–274.

Aydin, F.A.; Soylak, M.; (2007). Solid Phase Extraction and Preconcentration of Uranium(VI) and Thorium(IV) on Duolite XAD761 Prior to Their Inductively Coupled Plasma Mass Spectrometric Determination. Talanta, 72 (1): 187–192.

Babel, S.; Kurniawan, T.A.; (2003). Low-Cost Adsorbents for Heavy Metals Uptake from Contaminated Water: A Review. J. Hazard. Mater., 97 (1-3): 219-243.

Bakatula, E.N.; K.Mosai, A.; Hlanganani, T.; (2015). Removal of Uranium from Aqueous Solutions Using Ammonium-Modified Zeolite. S. Afr. J. Chem., 68: 165–171.

Bosco, L.M.; Jimenez, R.S.; Carvalho, W.A.; (2005). Removal of Toxic Metals from Wastewater by Brazilian Natural Scolecite. J. Colloid. Int. Sci., 281(2): 424–431.

Chisholm-Brause, C.J.; Berg, J.M.; Matzner, R.A.; Morris, D.E.; (2001). Uranium (VI) Sorption Complexes on Montmorillonite as a Function of Solution Chemistry. J Colloid. Interf. Sci., 233: 38-49.

Christian, T.C.V.; Fauduet, H.; Porte, C.; Delacroix, A.; (2003). Removal of Cd(II) and Pb(II) Ions, from Aqueous Solutions, by Adsorption onto Sawdust of Pinus Sylvestris. J. Hazard. Mater., 105 (1-3): 121-142.

Dabrowski, A.; Hubicki, Z.; Padkos´cielny, P.; Robens, E.; (2004). Selective Removal of the Heavy Metal ions From Waters and Industrial Wastewater by Ion-Exchange Method. Chemosphere., 56 (2): 91–106.

Dent, J.; Ramsay, J.D.F.; Swaanton, S.W.; (1992). An EXAFS Study of Uranyl Ion in Solution and Sorbed onto Silica and Montmorillonite Clay Colloids. J. Colloid. Interf. Sci., 150 (1): 45-60.

Dimirkou, A.; (2007). Uptake of Zn2+ Ions by a Fully Iron-Exchanged Clinoptilolite. Case Study of Heavily Contaminated Drinking Water Samples. Water Res., 41(12): 2763–2773.

Doula, M.; (2006). Removal of Mn2+ Ions from Drinking Water by Using Clinoptilolite and a Clinoptilolite–Fe Oxide System. Water Res., 40 (17): 3167–3176.

Doula, M.; Dimirkou, A.; (2008). Use of an Iron-Overexchanged Clinoptilolite for the Removal of Cu2+ Ions from Heavily Contaminated Water Samples. J. Hazard. Mater., 151 (2-3): 738–745.

Duff David, G.; Ross Sheina, M.C.; Vaughan, D.H.; (1988). Adsorption form Solution: An Experiment to Illustrate the Langmuir Isotherm. J. Chem. Ed., 65 (9): 815-816.

Dushenkov, S.; Vasudev, D.; Kapulnik, Y.; Gleba, D.; Fleisher, D.; Ting, KC.; Ensley, B.; (1997). Removal of Uranium from Water Using Terrestrial Plants. Environ. Sci. Technol., 31(12): 3468–3474.

El Aamrania, F.Z.; Durob, L.; De Pablo, J; Bruno, J.; (2002). Experimental Study and Modeling of the Sorption of Uranium (VI) onto Olivine-Rock. Appl. Geochem., 17 (4): 399-408.

Fathizadeh, M.; Aroujalian, A.; Raisi, A.; (2011). Effect of Added NaX Nano-Zeolite into Polyamide as a Top Thin Layer of Membrane on Water Flux and Salt Rejection in a Reverse Osmosis Process. J. Membr. Sci., 375 (1-2): 88–95.

Fan, F.L.; Qin, Z.; Bai, J.; Rong, W.D.; Fan, F.Y.; Tian, W.; Lei, X.W.; Wang, Y.; Zhao, .L.; (2012). Rapid Removal of Uranium from Aqueous Solutions Using Magnetic Fe3O4@SiO2 Composite Particles. J. Environ. Radioact., 106 (1): 40–46.

Freundlich, H.M.F.; (1906). User Die Adsorption in Losungen. Z. Phys. Chem., 57 (A): 385-470. Fungaro, A.D.; Yamaura, M.; Craesmeyer, R.G.; (2012). Uranium Removal from Aqueous Solution by Zeolite from Fly Ash-Iron Oxide Magnetic Nanocomposite. I.RE.CH.E., 4 (3): 2035-1755.

Gupta, A.R.; Venkataramani, B.; (1991). Effect of Anions on the Sorption of Uranyl Ions on Hydrous Oxides: Application of the Surface Hydrolysis Model. Colloids Surf., 53 (1): 1-19.

Gupta, V.K.; Ali, I.; (2004). Removal of Lead and Chromium from Wastewater Using Bagasse Fly Ashea Sugar Industry Waste. J Colloid. Interf. Sci., 271 (2): 321-328.

Hall, K.; Eagleton, L.; Andreas, A.; Theodore, V.; (1966). Pore and Solid-Diffusion Kinetics in Fixed-Bed Adsorption Under Constant-Pattern Conditions. Indus. Eng. Chem. Fund., 5 (2): 212-223.

Hasley, G.D.; (1952). The Role of Surface Heterogeneity. Adv. Catal., 4: 259-267.

Karadag, E.; Saraydin, D.; Guven, O.; (1995). Behaviors of Acrylamide/Itaconic Acid Hydrogels in Uptake of Uranyl Ions from Aqueous Solutions. Sep. Sci. Technol., 30 (20): 3747-3760.

Lagergern, S.; (1898). About the Theory of So-Called Adsorption of Soluble Substances. K Sven Vetenskapsakad Handl., 24 (4): 1–39.

Mahmood, S.N.; Naeem, S.; Basit, N.; Usmani, T.H.; (1993). Microbial Evaluation of Silver Coated/Impregnated Sand for Purification of Contaminated Water. Environ. Technol., 14 (2): 151-157.

Mahmoud, M.A.; (2013). Removal of Uranium (VI) from Aqueous Solution using Low Cost and Eco-Friendly Adsorbents. J. Chem. Eng. Process Technol., 4(6): 1-4 .

Mar Camacho, L.; Deng, Sh.; Parra, R.R.; (2010). Uranium Removal from Groundwater by Natural Clinoptilolite Zeolite: Effects of pH and Initial Feed Concentration. J. Hazard. Mater., 175 (1–3): 393–398.

Matsumura, Y.; Yoshikata, K.; Kunisaki, S.I.; Tsuchido, T.; (2003). Mode of Bactericidal Action of Silver Zeolite and its Comparison with that of Silver Nitrate. Appl. Environ. Microbiol., 69 (7): 4278-4281. doi: 10.1128/AEM.69.7.4278-4281.2003.

Mckay, Y.S.G.; (1998). The Kinetics of Sorption of Basic Dyes from Aqueous Solution by Sphagnum Moss Peat. Can. J. Chem. Eng., 76 (4): 822–827.

Mellah, A.; Chegrouche, S.; Barkat, M.; (2006). The Removal of Uranium(VI) from Aqueous Solutions onto Activated Carbon: Kinetic and Thermodynamic Investigations. J. Colloid. Interf. Sci., 296 (2): 434-441.

Michard, P.; Guibal, E.; Vincent, T.; Cloirec, P.L.; (1996). Sorption and Desorption of Uranyl Ions by Silica Gel: pH, Particle Size and Porosity Effects. Micro. Mater., 5 (5): 309-324.

Milja, T.E.; Prathish, K.P.; Rao, T.P.; (2011). Synthesis of Surface Imprinted Nanospheres for Selective Removal of Uranium from Simulants of Sambhar Salt Lake and Ground Water. J. Hazard. Mater., 188 (1-3): 384–390.

Monoj, K.M.; (2010). Removal of Pb(II) from Aqueous Solution by Adsorption Using Activated Tea Waste. Korean. J. Chem. Eng., 27 (1): 144-151.

Nangmenyi, G.; Yue, Z.; Mehrabi, S.; Mintz, E.; Economy, J.; (2009). Synthesis and Characterization of Ag Nanoparticle Impregnated Fiberglass and Utility in Water. Disinfection. Nanotechnol., 20 (49): 495-505.

Nriagu, J.; Nam, D. H.; Ayanwola, T. A.; Dinh, H.; Erdenechimeg, E.; Ochir, C.; Bolorma, T.A.; (2012). High Levels of Uranium in Groundwater of Ulaanbaatar. Mongolia. Sci. Total. Environ., 414 (1): 722–726.

Pouretedal, H.R.; Ahmadi, M.; (2013). Preparation, Characterization and Determination of Photocatalytic Activity of MCM-41/ZnO and MCM-48/ZnO Nanocomposites. Iran. J. Catal., 3 (3): 149-155.

Runping, H.; Weihua, Z.; Wang, Y.; Zhu, L.; (2007). Removal of Uranium(VI) from Aqueous Solutions by Manganese Oxide Coated Zeolite: Discussion of Adsorption Isotherms and pH Effect. J. Environ. Radioact., 93 (3): 127-143.

Sadeghi, M.; Yekta, S.; Babanezhad, E.; (2014). MnO2-AgX Zeolite Nanocomposite as an Adsorbent Catalyst for the Decontamination against Sulfur Mustard Simulants. Caspian J. Chem., 3 (1): 57-75.

Sadeghi, M.; Ghaedi, H.; Yekta, S.; Babanezhad, E.; (2016). Decontamination of Toxic Chemical Warfare Sulfur Mustard and Nerve Agent Simulants by NiO NPs/Ag-Clinoptilolite Zeolite Composite Adsorbent. J. Environ. Chem. Engineering, 4: 2990–3000.

Sadeghi, S.; Azhdari, H.; Arabi, H.; Zeraatkar Moghaddam, A.; (2012). Surface Modified Magnetic Fe3O4 Nanoparticles as a Selective Sorbent for Solid Phase Extraction of Uranyl Ions from Water Samples. J. Hazard. Mater., 215– 216 (1): 208–216.

Satpati, S.K.; Pal, S.; Goswami, D.; Tewari, P.K.; Roy, S.B.; (2015). Extraction of Uranium from Nuclear Industrial Effluent Using Polyacrylhydroxamic Acid Sorbent. Int. J. Environ. Sci. Technol., 12: 255–262.

Schmeide, K.; Pompe, S.; Bubner, M.; Heise, K.H.; Bernhard, G.; Nitsche, H.; (2000). Uranium(VI) Sorption onto Phyllite and Selected Minerals in the Presence of Humic Acid. Radiochim. Acta., 88 (9-11): 723-728.

Semiao, J.C.; Rossiter, M.A.; H. Schafer, I. A.; (2010). Impact of Organic Matter and Speciation on the Behaviour of Uranium in Submerged Ultrafiltration. J. Membr. Sci., 348 (1-2): 2174–180.

Sidhu, SH.; Keith-Roach, M.J.; Lloyd, J.R.; Vaughan, D.J.; (2010). A Review of the Environmental Corrosion, Fate and Bioavailability of Munitions Grade Depleted Uranium. Sci. Total. Environ., 408 (23): 5690–5700.

Shinde, N.R.; Bankar, A.V.; Kumar, A.R.; Zinjarde, S.S.; (2012). Removal of Ni (II) ions From Aqueous Solutions by Biosorption onto Two Strains of Yarrowia Lipolytica. J. Environ. Manag., 102 (1): 115–124.

Singh, B.; Garg, V.K.; Yadav, P.; Kishore, N.; Pulhani, V.; (2014). Uranium in Groundwater from Western Haryana. J. Radioanal. Nucl. Chem., 301 (2): 427–433.

Stephanie, E.S.; Smith, Sullivan, K.A.; (1999). Organic Transformations Using Zeolites and Zeotype Materials. Tetrahedron., 55 (1): 12657–12698.

Temkin, M.I.; (1941). Adsorption Equilibrium and Kinetics of Processes on Non-Homogeneous Surface and in the Interaction between Adsorbed Molecules. Zh. Fiz. Chim., 15: 296-332.

Teymouri, M.; Samadi-Maybodi, A.; Vahid, A.; (2011). A Rapid Method for the Synthesis of Highly Ordered MCM-4. Int. Nano Lett., 1 (1): 34-37.

Wazne, M.; Korfiatis, G.P; Meng, X.; (2003). Carbonate Effects on Hexavalent Uranium Adsorption by Iron Oxyhydroxide. Environ. Sci. Technol., 37 (16): 3619-3624.

AUTHOR (S) BIOSKETCHES

Sina Yekta, M.Sc., Instructor, Department of Chemistry, Qaemshahr Branch, Islamic Azad University, Qaemshahr, Iran, *Email: sina.yekta.chem@gmail.com*

Meysam Sadeghi, Ph.D., Department of Chemistry, Lorestan University, Khorramabad, Iran

Hamed Ghaedi, Ph.D., Assistant Professor, Department of Chemistry, Bushehr Branch, Islamic Azad University, Bushehr, Iran

Nooshin Shahabfar, M.Sc., Department of Nuclear Engineering, Radiation Application, Amir Kabir University, Tehran, Iran